^1H and ^{13}C NMR Relaxation Investigation of the Calcium Complex of β-Alanyl-L-Histidine (Carnosine) in Aqueous Solution

Elena Gaggelli *
Department of Chemistry, University of Siena, 53100 Siena, Italy
Gianni Valensin
Institute of Chemistry, University of Basilicata, 85100 Potenza, Italy

^{13}C and ^1H NMR chemical shifts, J couplings, and spin–lattice relaxation rates were measured for carnosine in aqueous solution at pH 7.0. A Dreiding model of the 'most-probable' conformation was built up, showing predominance of the g^- rotamer and folding of the β-alanyl moiety towards the imidazole ring. The structural and dynamic picture was shown not to be severely changed by stepwise titration with Ca^{II} ions. Exchange of carnosine among the bulk solution, a monomer complex (Ca^{2+} liganded by carboxy and carbonyl oxygens) and a dimer complex (Ca^{2+} liganded also by imidazole nitrogen) was suggested. The formation constant was evaluated at *ca.* 25 dm^3 mol^{-1}. A Dreiding model of the dimeric complex was also built up on the basis of measured cross-relaxation terms of proton pairs, showing occurrence of intermolecular interactions between peptide molecules mediated by Ca^{II} ions.

Carnosine (*N*-β-alanyl-L-histidine) is a naturally occurring dipeptide (Figure 1) found in high concentration (in the range 1–4 mmol dm^{-3}) in muscle and in the olfactory bulb of man and of several animals.[1] Related imidazolyl dipeptides, such as anserine (*N*-β-alanyl-1-methyl-L-histidine) and homocarnosine (γ-aminobutyryl-L-histidine), also occur in the excitable tissues of many species.[2] It is generally accepted that carnosine and its analogues are involved in the physiology of the specialized tissues where they are found. Several reports have appeared about involvement of carnosine in regulation of anaerobic glycolysis of skeletal muscle,[3] in olfactory neurotransmission[4] and, possibly, in wound healing.

The inhibition of carnosinase activity in many tissues by chelating agents, such as EDTA, *o*-phenanthroline and 8-hydroxyquinoline-5-sulphonic acid,[5] justifies extensive investigation of metal–carnosine complexation equilibria. Paramagnetic divalent metal ions, especially copper, have been given a great prominence,[6–13] due to the relatively easy approach offered by magnetic resonance spectroscopic techniques. However, the need to keep the metal concentration at or below metal:ligand ratios of *ca.* 10^{-3}–10^{-4}, has limited the investigation of the effects of metal complexation upon conformational equlibria within the highly flexible peptide molecule.

The aim of this paper is to characterize the conformation and molecular dynamics of carnosine in aqueous solution in the physiological range of pH, and to delineate how the ubiquitous diamagnetic Ca^{II} ions affect them. ^{13}C spin–lattice relaxation rates, and selective ^1H spin–lattice relaxation rates have been used in order to extract geometrical and dynamic features of well-defined hetero- or homo-nuclear spin pairs.

Experimental

Carnosine was supplied by Sigma Chemical Co. and used without further purification. Calcium chloride was a product of Bracco Merck. Solutions were made in D_2O (99.95% from Merck) and the pH was adjusted with DCl or NaOD. Concentrations of Ca^{2+} were determined by complexometry with EDTA (from Sigma).

^{13}C and ^1H NMR spectra were obtained on a Varian XL-200 spectrometer operating at 50.3 and 200 MHz respectively.

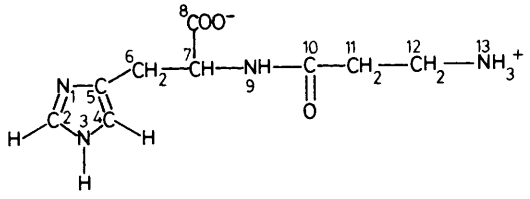

Figure 1.

Chemical shifts were determined by using sodium [2,2,3,3-$^2H_4$]-3-trimethylsilylpropanoate (from Wilmad) as an internal reference standard. ^{13}C-{^1H} NOEs were determined by recording broadband and gated decoupled carbon spectra.

Non-selective spin–lattice relaxation rates were measured by using the inversion–recovery pulse sequence. Selective and double-selective proton spin–lattice relaxation rates were measured by using inversion–recovery pulse sequences where the 180° pulse was given by the proton decoupler switched on at selected frequencies for relative long times.[14–16] Typical experimental settings were 21 dB decoupler power attenuation and 21 ms for the 180° pulse. The values of the spin–lattice relaxation rate were calculated in the initial rate approximation[14] with a three-parameter exponential regression analysis of the recovery curves of the longitudinal magnetization components.

Results and Discussion

Conformational Dynamics of Carnosine in Solution.—^{13}C NMR spin–lattice relaxation rates are reported in Table 1 for carnosine (0.2 mol dm^{-3}), in the absence and in the presence of different concentrations of Ca^{II} ions. The ^{13}C chemical shifts of carnosine in aqueous solution were shown to be independent of concentration in the range 1–200 mmol dm^{-3}, and so intermolecular interactions could be neglected.

The ^{13}C-{^1H} NOE's were found at almost the maximum value of 2.99 for either protonated or non-protonated carbons, thus demonstrating that the ^{13}C–^1H dipole–dipole interaction is the dominant relaxation mechanism and also that the correlation times for modulation of each relaxation vector are expected to occur within the extreme narrowing region.

Table 1. Chemical shifts and ^{13}C spin–lattice relaxation rates for carnosine 0.2 mol dm^{-3} in D_2O at pH 7.0 at increasing concentration of Ca^{2+} ions.

		R_1/s^{-1} [a]			
	δ (ppm)	$[Ca^{2+}]$/mol dm^{-3} 0	0.05	0.2	0.4
C-2	135.7	1.264	1.462	1.742	1.715
C-5	133.2	0.138	0.143	0.155	0.277
C-4	117.4	0.747	0.825	1.091	1.404
C-6	29.0	2.217	2.361	2.564	2.586
C-7	55.2	1.159	1.412	2.088	2.091
C-8	177.9	0.118	0.106	0.084	0.138
C-10	171.6	0.070	0.074	0.095	0.099
C-11	35.8	1.592	1.487	1.325	1.086
C-12	32.3	0.759	0.982	1.490	1.302

[a] Errors in R_1 measurements were evaluated at ±5% confidence limits of the regression analysis.

Table 2. ^1H NMR chemical shifts, non-selective (R^{ns}) and selective (R^s) spin–lattice relaxation rates, and F ratios (R^{ns}/R^s) for carnosine 0.2 mol dm^{-3} in D_2O at pH = 7.0.

Resonance	R^{ns}/s^{-1} [a]	R^s/s^{-1} [a]	F	δ (ppm)
2-H	0.567	0.576	0.984	6.93
4-H	0.579	0.540	1.072	6.17
7-H	0.473	0.342	1.384	3.71
11-H	1.098	1.067	1.029	2.44
6-H	2.326	—	—	2.37
6′-H	2.326	—	—	2.21
12-H	1.125	1.076	1.045	1.88

[a] Errors in R^{ns} or R^s measurements were evaluated at ±5% confidence limits of the regression analysis.

Table 3. Coupling constants in the ABX spin system CH–βCH_2 of carnosine, 0.2 mol dm^{-3} at pH 7.0 and fractional populations P of g^-, t, and g^+ rotamers as a function of Ca^{2+} concentration.

	$[Ca^{2+}]$/mol dm^{-3}				
	0	0.05	0.1	0.2	0.4
J_{AB} [a]	15.40	15.10	14.92	14.81	14.46
J_{AX} [a]	4.90	4.61	4.57	4.90	4.85
J_{BX} [a]	8.60	9.09	9.04	8.78	8.85
P_I	0.586	0.640	0.635	0.647	0.650
P_{II}	0.147	0.107	0.112	0.126	0.133
P_{III}	0.267	0.253	0.253	0.227	0.217

[a] Coupling constants J measured in Hz.

Inspection of ^{13}C spin–lattice relaxation rates (Table 1, second column) showed that, among the protonated carbons, C-2, C-6, and C-7 have approximately the same reduced relaxation rate (R_1/n_H where n_H is the number of protons attached to the carbon), whereas C-4, C-11, and especially C-12 display much slower rates. Although interpretation of the ^{13}C spin–lattice relaxation rates can be complicated, in this particular case the solution dynamics can be visualized in terms of a main rotational reorientation around a molecular axis passing through or parallel to C-2, C-6, and C-7, coupled with segmental motion of the amino-terminal peptide moiety and librational motion of the imidazole ring. The correlation time of the principal rotation can be evaluated by using the Allerhand's formula[17] for isotropic motions within the extreme narrowing region. By considering 1.09 Å as the r_{C-H} distance (a typical value obtained from rotational spectroscopy) τ_R = 58 ps at 295 K was calculated. Since extreme narrowing conditions hold, that is to say the R_1 values are far away from the maximum of the R_1 *vs.* τ_R curve, the calculated τ_R is not expected to be severely affected by the setting of r_{C-H}.[18]

The correlation time for internal motion of the imidazole ring around the rotational axis can be calculated by considering the equations given by Woessner for the effect of internal motion on the relaxation of a group attached to a body undergoing isotropic motion.[19] Taking the relaxation rate of C-4 into account, and considering 144° as the angle between the C-4/4-H vector and the axis of internal reorientation, yielded τ_G = 12 ps at 295 K for the correlation time for internal motion of the C-4/4-H relaxation vector and, as a consequence, $\tau_{||}$ = 9.9 ps at 295 K for the total correlation time for reorientation of the C-5/5-H vector ($\tau_{||}^{-1} = \tau_R^{-1} + \tau_G^{-1}$).[17]

Interpretation of ^1H spin–lattice relaxation rates is usually much more difficult because of occurrence of several relaxation mechanisms involving many relaxation vectors. Such interpretation can be greatly simplified by using selective irradiation methods.[15,16] In fact, measuring the ratio, F, between non-selective (R^{ns}) and selective (R^s) relaxation rates provides a means of estimating the relevance of the ^1H–^1H dipole–dipole interaction in determining the relaxation mechanism.[12]

Since the F value for 7-H (Table 2) approaches the theoretical value of 1.5,[12] it can be reasonably stated that the dipolar interaction provides the relaxation mechanism for the 7-H/6-H, and, most probably, for the 11-H/12-H relaxation vectors, where selective excitation cannot succeed in 'washing out' cross-relaxation terms between protons having the same chemical shift. This being the case, equations (1) and (2) are valid,[16,20]

$$R_i^{ns} = \sum_{i \neq j} \rho_{ij} + \sum_{i \neq j} \sigma_{ij} \quad (1)$$

$$R_i^{s} = \sum_{i \neq j} \rho_{ij} \quad (2)$$

where ρ_{ij} and σ_{ij} are the direct- and the cross-relaxation terms for any proton pair and the sum is extended to all the interacting dipole pairs. ρ_{ij} and σ_{ij} are given by equations (3) and (4)

$$\rho_{ij} = \gamma_H^4 \hbar^2 \tau_c / r_{ij}^6 \quad (3)$$

$$\sigma_{ij} = \rho_{ij}/2 \quad (4)$$

where r_{ij} is the proton–proton distance, τ_c is the motional correlation time, γ_H is the magnetogyric ratio, $\hbar$ is the reduced Planck constant. The statement of equations (3) and (4) is based on the assumption that extreme narrowing conditions hold. Since the proton pairs involved in dipole interactions are not at fixed distance the r_{ij} occuring in equations (3) and (4) should be interpreted as an average distance, weighted over the N discrete conformational sites among which the molecule may exchange.[21]

By using the correlation time calculated from ^{13}C relaxation data and by considering 1.75, 2.47, and 3.07 Å as the proton–proton distances of two geminal, *gauche*, and *trans* protons, respectively, it was possible to calculate ρ and σ terms in the three cases: ρ_{gem} = 1.149 s^{-1}, σ_{gem} = 0.574 s^{-1}, ρ_g = 1.146 s^{-1}, σ_g = 0.073 s^{-1}, ρ_t = 0.040 s^{-1}, σ_t = 0.020 s^{-1}. A comparison was then possible between experimental (Table 2) and theoretical relaxation rates, indicating that the preferred conformation is one with the two 6-H protons *gauche* to the 7-H. Such conclusions ratify the J analysis within the ABX pattern, as shown in Table 3. The J_{AX} and J_{BX} values can be used to

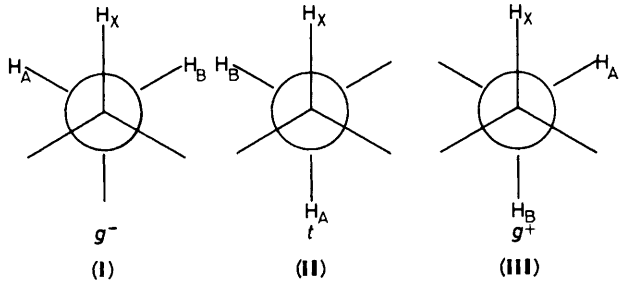

Figure 2. Minimum-energy staggered conformations around the (C-6)–(C-7) bond of carnosine. H_x denotes the 7-H proton, H_A and H_B the 6-H and 6′-H protons.

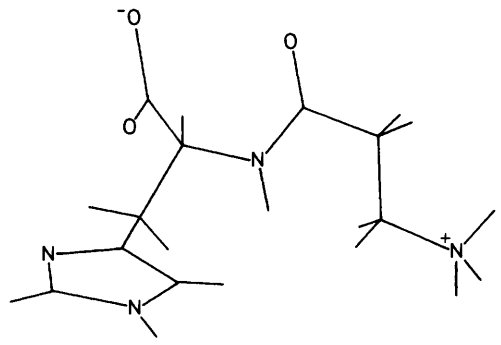

Figure 3. Projection of the Dreiding model of the 'most probable' conformation of carnosine in aqueous solution.

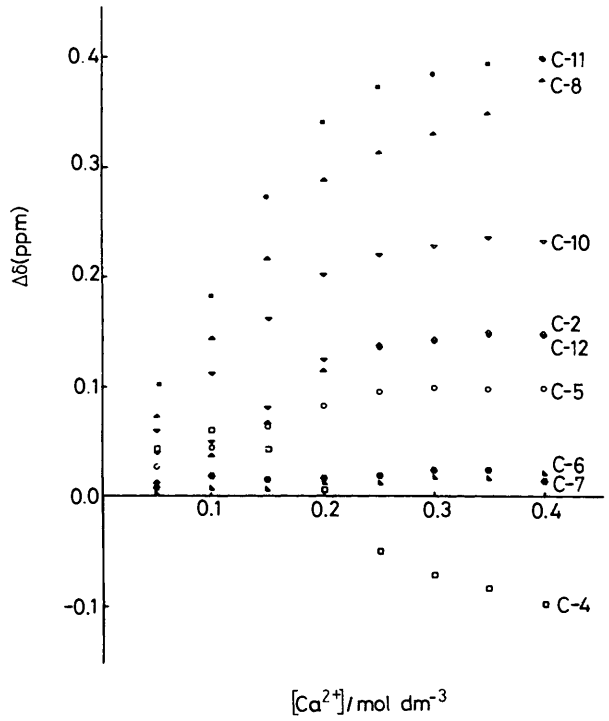

Figure 4. Concentration dependence of Ca^{2+}-induced ^{13}C chemical shifts of carnosine, 0.2 mol dm^{-3} in aqueous solution at pH 7.0. Positive values of Δδ denote downfield shifts.

Table 4. Calculated cross-relaxation terms σ_{ij} for carnosine 0.2 mol dm^{-3} in D_2O at pH 7.0 in the presence of different Ca^{2+} concentrations.

	$[Ca^{2+}]$/mol dm^{-3}				
σ_{ij}/s^{-1}	0	0.05	0.1	0.2	0.4
$\sigma_{4,12}$	0.025	0.014	0.008	—	—
$\sigma_{11,12}$	0.021	0.022	0.024	0.032	0.034
$\sigma_{2,11}$	—	—	—	0.010	0.017
$\sigma_{2,12}$	—	—	0.004	0.006	0.007
$\sigma_{5,7}$	—	—	—	0.004	0.017
$\sigma_{5,11}$	—	—	0.010	0.013	0.014
$\sigma_{7,11}$	—	—	—	0.009	0.013
$\sigma_{7,12}$	—	—	0.009	0.009	0.019

calculate fractional populations of the three minimum-energy staggered conformations shown in rotamers (**I**) to (**III**) in Figure 2. Such a method of conformational analysis, however, is very strongly dependent on equations that relate the measured averaged vicinal coupling constants to those found in the rotamers, weighted according to their fractional populations. By using the equations given by Feeney for the rotamer couplings within αCH–βCH$_2$ proton multiplets of amino-acid sidechains,[22] the fractional populations reported in the first column of Table 3 were evaluated, yielding evidence of preferential occurrence of the g^- rotamer.

Further information about geometric and dynamic features of carnosine could be obtained by measuring ^1H spin–lattice relaxation rates following selective irradiation of predefined resonance pairs. The relaxation rate of any proton i after irradiation of any resonances i and k is given by equation (5)[15,16] where the first term on the right-hand side is the

$$R_i^{ik} = \sum_{i \neq j} \rho_{ij} + \sigma_{ik} \qquad (5)$$

selective relaxation rate of proton i [equation (2)]. Therefore, the cross-relaxation term of any proton pair can be measured by the difference between the double-selective and the selective relaxation rates. By measuring the double-selective relaxation rates for all the possible proton pairs of carnosine (with the exception of those involving 6-H and 6′-H), the terms reported in the first column of Table 4 were evaluated.

Apart from the obvious σ term between protons within the β-alanyl moiety, only a cross-relaxation term between 4-H and the 12-H methylene protons was detected, and this was taken as providing evidence of folding of the β-alanyl chain towards the imidazole ring. As σ is a function of only one distance and only one correlation time, a geometric or dynamic interpretation of the observed σ values could be attempted [equations (3) and (4)]. Hence, an average distance of 2.20 Å was evaluated for the 4-H/12-H relaxation vector, by using the total correlation time calculated from ^{13}C relaxation rate of C-4. In the same way, knowledge of $\sigma_{11,12}$ allowed evaluation of σ_{gem} for the 11-H protons and hence of the corresponding correlation time (τ_c = 34 ps at 295 K). If the *gauche* distance is considered as the average distance between one 11-H proton and one 12-H proton, a correlation time of 16 ps at 295 K is calculated for modulation of the 11-H/12-H vector. All the NMR results could be used to build a Dreiding model of the 'most-probable' conformation in solution, as shown in Figure 3 as a projection in the plane of the figure.

Binding Sites for Calcium and Association Features.—The conversion of the free form of carnosine to the Ca^{2+} complex yields changes in the ^{13}C NMR shifts, while not severely perturbing the ^1H NMR spectrum. The dependence of ^{13}C chemical shifts upon concentration of Ca^{2+} ions is shown in Figure 4 as a plot of Δδ *vs.* $[Ca^{2+}]$. These titration curves show that, on stepwise titration with $CaCl_2$, six of the nine resonances are deshielded to different extents, in the order C-11 ≃ C-8 > C-10 > C-2 = C-12 > C-5. The C-7 and C-6 resonances are

Table 5. Geometrical constants and correlation times for internal reorientation of C-5/5-H and C-2/2-H vectors as a function of θ, the angle between the C–H vector and the axis of internal reorientation.[a]

				τ_G(C-5)	τ_G(C-2)
θ	A	B	C	ps	ps
15	0.81	0.19	0.00	i[b]	4.5
30	0.39	0.56	0.05	4.6	20.5
45	0.06	0.75	0.19	12.1	29.8
60	0.02	0.56	0.42	16.8	42.1
75	0.16	0.19	0.65	20.7	73.4
90	0.25	0.00	0.75	23.3	101.0

[a] See text for further details. [b] Imaginary root of the equation.

not affected by the presence of Ca^{2+} while the C-4 resonance is deshielded at low concentrations and shielded at high Ca^{2+} concentrations. The observed shifts suggest that the rate of interconversion between free and bound carnosine is fast on the experimental time scale. It is apparent that the titration curves of C-11, C-8, and C-10, as well as those of other carbons, display a change in slope around $[Ca^{2+}] = 0.2$ mol dm^{-3}, *i.e.* at a ligand : metal ion ratio of 1.0, thus indicating a 1 : 1 stoicheiometry for the complex in D_2O.

Assumption of this stoicheiometry and consideration of the limiting chemical shifts for bound carnosine (Figure 4) led to an approximate value for the association constant by using the observed (exchange-averaged) chemical shifts at intermediate Ca^{2+} concentrations.[23] For $[Ca^{2+}]/[\text{carnosine}] = 0.75$, the values obtained for the molar fraction of bound carnosine were 0.49 ± 0.03, 0.52 ± 0.04, and 0.56 ± 0.03, using C-11, C-8, and C-10 signals respectively. These led to an average K_f of approximately 25 dm^3 mol^{-1}.

As far as the structure of the complex is concerned, the observed shifts provide substantial evidence that carboxy and carbonyl oxygens are the groups responsible for metal binding, with consequent deshielding of the ^{13}C resonances. However the downfield shifts experienced by ring carbons and particularly the upfield shift of C-4 resonance at high Ca^{2+} concentrations are not likely to arise because of Ca^{2+} binding to the oxygens, especially if it is considered that C-6 and C-7 are not affected by the complexation process. One of the following events can be therefore suggested to occur alternatively, (a) a change in conformation upon metal binding, (b) binding of Ca^{2+} to a secondary site localized on the imidazole ring, or (c) occurrence of intermolecular interactions mediated by Ca^{II} ions.

Since relaxation rates of ^{13}C as well as of ^1H nuclei were shown to allow the elucidation of certain conformational features of carnosine in solution, the same was expected to hold for the Ca^{2+} complex, which should provide information on the molecular changes brought about by Ca^{2+} complexation.

Conformational Dynamics of the Ca^{2+}/Carnosine 1:1 *Complex.*—The appearance of the ^1H NMR spectrum does not change upon addition of Ca^{II} ions up to a 2:1 metal:ligand ratio. The ^1H resonances undergo very small downfield shifts (maximum 0.03–0.05 ppm), but the spin patterns remain the same. The ABX part of the spectrum, as shown in Table 3, remains practically unaffected, with the exception of a certain decrease in the J_{AB} coupling constant and a slight redistribution of fractional populations of rotamers around the (C-6)–(C-7) chemical bond. The addition of Ca^{II} ions brings about a further increase in the fractional population of the g^- rotamer that seems to be the most favoured for metal complexation.

From the dynamic point of view, stepwise titration with $CaCl_2$ causes increase in all the ^{13}C relaxation rates except that of C-11, as shown in Table 1. Within the extreme-narrowing region, such an increase is consistent with a slowing down of the molecular motions responsible for modulation of the ^{13}C–^1H relaxation vectors. At Ca^{2+} concentrations lower than or equal to 0.05 mol dm^{-3} the dynamic picture is quite similar to that observed for carnosine in solution; the relaxation rates of C-2, C-6, and C-7 are coherent with an almost isotropic reorientation around a molecular axis passing through these three carbons, the imidazole ring undergoes a certain degree of internal motion, and the β-alanyl moiety shows features typical of segmental motion. At Ca^{2+} concentrations higher than 0.05 mol dm^{-3} the properties of the Ca^{2+}-complex start prevailing on those of the free ligand. By considering the ^{13}C relaxation rates at $[Ca^{2+}] = 0.2$ mol dm^{-3} it can be readily observed that it is no more possible to detect principal motion around any molecular axis. The largest reduced relaxation rate is that of C-7, the relaxation vector of which, C-7/7-H, can be evaluated to be modulated with a correlation time $\tau_c = 100$ ps at 295 K,[17] which is almost twice of that found for the main reorientational motion of free carnosine in solution.

Since the axis of the main reorientational motion is not known in this case, the Woessner model cannot be directly applied to evaluate correlation times for internal motions. However the following considerations allow one to infer some dynamic features of the complex. According to the method of Woessner the correlation function within the extreme narrowing region is given by equation (6) where $1/\tau_B = 1/\tau_R +$

$$f(\tau) = A\tau_R + B\tau_B + C\tau_C \qquad (6)$$

$1/6\tau_G$; $1/\tau_C = 1/\tau_R + 2/3\tau_G$; $A = 0.25\ (3\cos^2\theta - 1)^2$; $B = 3\sin^2\theta\cos^2\theta$; $C = 0.75\sin^4\theta$.

In these equations θ is the angle between the C–H vector and the axis of reorientation, τ_R the correlation time for the main rotational motion and τ_G that for internal motion. By considering the ^{13}C relaxation rates of C-2 and C-4, the function of τ_G *vs.* θ can be built up for both carbons as shown in Table 5. It can be readily observed that the two carbons possess the same τ_G when the two θ angles between the C–H vectors and the axis of internal reorientation are 45° out of phase. This strongly suggests that such axis passes through C-5 and intersects the (N-3)–(C-2) chemical bond. Therefore carnosine assumes a conformation, in the metal-bound state, such that the β-alanyl moiety is moved away from the imidazole ring, and this also contributes to the observed chemical shifts within the β-alanyl moiety and the imidazole ring.

Since binding by Ca^{II} ions is not expected to yield relevant changes in motional correlation times, the calculated increase in both principal and internal correlation times is very likely to be determined by the presence of a certain amount of a dimeric complex with two Ca^{II} ions bound to two carnosine ligands. Such a complex will be in rapid exchange with the monomer and the bulk ligand, and its formation will favour certain intermolecular interactions. Thus the observed shifts within the imidazole moiety can be explained by the involvement of this group in the metal binding in the dimeric complex, and also by the occurrence of intermolecular interactions. It is observed that the greatest changes in ^1H chemical shifts (about 0.05 ppm downfield) are displayed by β-alanyl 12-H protons and by imidazole protons. These findings are supported by the fact that, at physiological pH, carnosine forms a similar dimeric complex with Cu^{II} ions,[6,10,11,13] (although the biological significance of such complex is not expected to be relevant).

The analysis of ^{13}C relaxation rates and shifts is confirmed by consideration of changes in ^1H relaxation rates induced by the stepwise addition of C^{II} ions, shown in Figures 4 and 6.

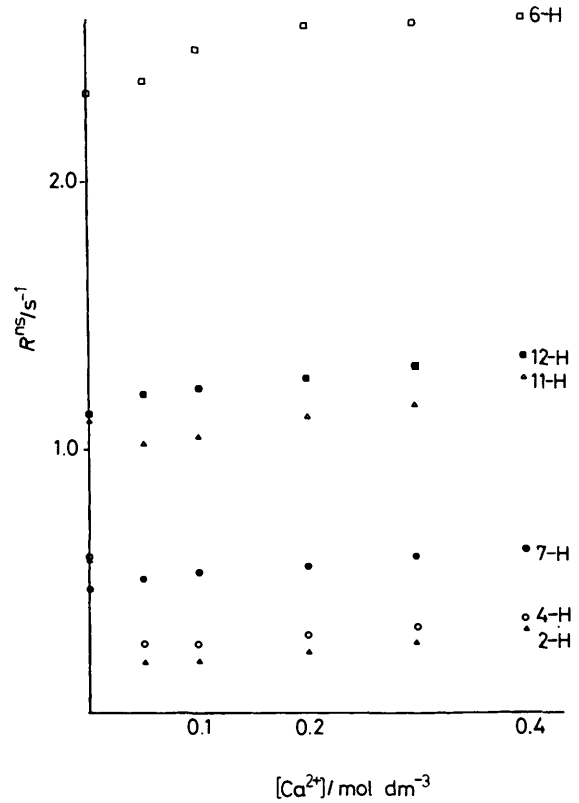

Figure 5. Dependence of R^{ns} upon Ca^{2+} concentration for protons of carnosine, 0.2 mol dm^{-3} in aqueous solution at pH 7.0.

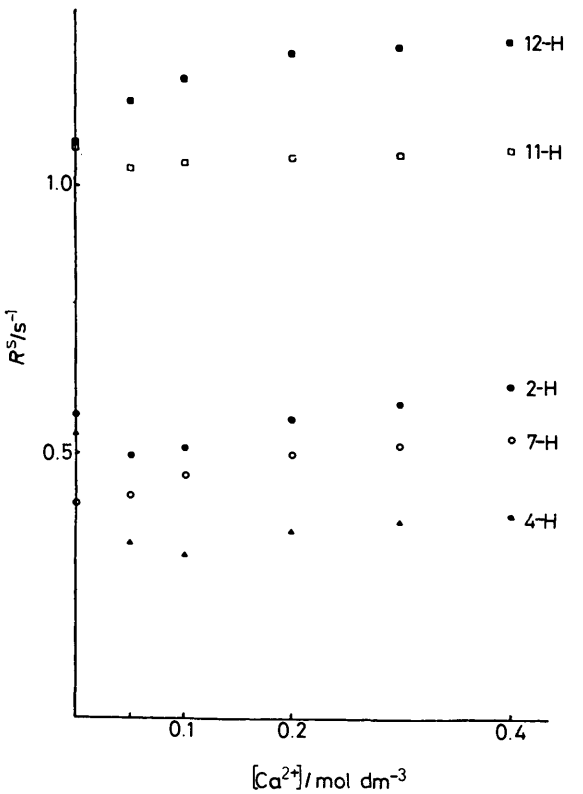

Figure 6. Dependence of R^{s} upon Ca^{2+} concentration for protons of carnosine, 0.2 mol dm^{-3} in aqueous solution at pH 7.0.

Two different trends can be detected in the behaviour of either R^{ns} or R^{s} at increasing Ca^{2+} concentration. 6-H, 12-H, and 7-H show a smooth continuous increase in the relaxation rate that seems to have reached its limiting value at $[Ca^{2+}] = 0.4$ mol dm^{-3}, whereas 11-H, 2-H, and 5-H display an initial decrease and a minimum at *ca.* $[Ca^{2+}] = 0.05$ mol dm^{-3}. Given that a relaxation rate, either non-selective or selective, of any proton is determined by a sum of pairwise ^1H–^1H dipole–dipole interactions, and that motional correlation times get longer on stepwise titration with Ca^{II} ions, it can be reasonably concluded that a decrease in R^{ns} or R^{s} is caused by a decrease in the number of actual spin pairs contributing to the relaxation rate. Therefore, in the same way, enhancement of R^{ns} or R^{s} reflects the lengthening of the motional correlation times and, occasionally, an increase in the number of contributing pairwise interactions.

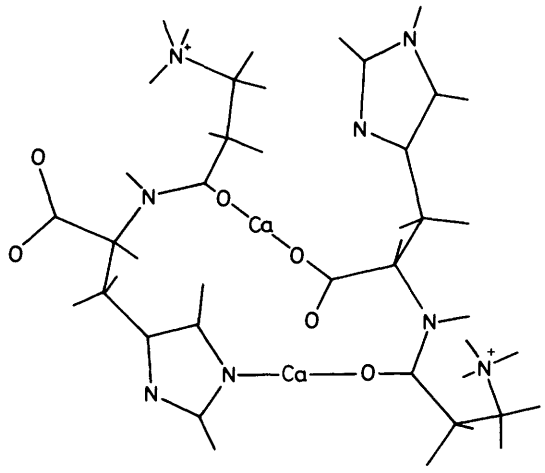

Figure 7. Projection of the Dreiding model of the calcium^{II} complex of carnosine in aqueous solution.

A more detailed picture can be attempted on the basis of calculated σ terms between defined proton pairs in the complex in solution. Consideration of cross-relaxation rates in Table 4 clearly demonstrates: (i) the disappearance of the 4-H/12-H cross-relaxation term as a consequence of a change in conformation, (ii) the increase in the 11-H/12-H cross relaxation term, reflecting a slowing down of molecular motions, and (iii) the appearance of cross-relaxation terms other than those observed for the free molecule in solution, that can be only accounted for by considering intermolecular interactions in a dimeric complex.

Conclusions

Carnosine forms, at pH 7.0, both monomeric and dimeric complexes with Ca^{II} ions, having an overall stability constant such that, at equimolar concentrations, about 50% of carnosine is bound. The carboxy and carbonyl oxygens are the binding groups in the monomer, whereas the imidazole nitrogen is involved in the dimeric complex together with one carboxy and one carbonyl oxygens of two different peptide molecules. Intermolecular interactions are promoted by dimer formation, as strongly suggested by the observed shifts and ^1H cross-relaxation terms between protons in different moieties of carnosine. Formation of the complex brings about slight structural rearrangements within the peptide, but it can be reasonably stated that the ligand assumes such a conformation in solution that metal binding does not require a conformational selection step.

The NMR results allow a Dreiding model to be built showing the most probable structure for free carnosine in solution (Figure 3); in the same way, a Dreiding model of the dimeric complex can be obtained. This type of model does not allow

accurate quantitation of the geometry of the complex, but does provide some representation of the intermolecular interactions that are likely to occur, which allows a structure to be proposed for the dimeric complex (Figure 7).

The presence of Ca^{II} ions and carnosine at high concentrations in several tissues suggests that the carnosine/Ca^{2+} complex may be very important from the biological point of view.

References

1 F. L. Margolis, *Science*, 1974, **184**, 909.
2 C. E. Brown, F. L. Margolis, T. H. Williams, R. G. Pitcher, and G. J. Elgar, *Arch. Biochem. Biophys.*, 1979, **193**, 529.
3 C. L. Davey, *Arch. Biochem. Biophys.*, 1960, **296**, 89.
4 P. Bessman and R. Baldwin, *Science*, 1962, **135**, 789.
5 A. Rosenberg, *Arch. Biochem. Biophys.*, 1960, **88**, 83.
6 H. C. Freeman and J. T. Szymanski, *Acta Cryatallogr.*, 1967, **22**, 406.
7 R. E. Viola, C. R. Hartzell, and J. J. Villafranca, *J. Inorg. Biochem.*, 1979, **10**, 281.
8 R. E. Viola, C. R. Hartzell, and J. J. Villafranca, *J. Inorg. Biochem.*, 1979, **10**, 293.
9 C. E. Brown and W. E. Antholine, *Biochem. Biophys. Res. Commun.*, 1979, **88**, 529.
10 C. E. Brown and W. E. Antholine, *J. Phys. Chem.*, 1979, **83**, 3314.
11 C. E. Brown and W. E. Antholine, *J. Chem. Soc., Dalton Trans.*, 1980, 590.
12 C. E. Brown, *J. Am. Chem. Soc.*, 1982, **104**, 5608.
13 C. E. Brown, D. Warren Vidrine, R. L. Julian, and W. Froncisz, *J. Chem. Soc., Dalton Trans.*, 1982, 2371.
14 R. Freeman, H. D. Hill, B. L. Tomlinson, and L. D. Hall, *J. Chem. Phys.*, 1974, **61**, 4466.
15 L. D. Hall and H. D. W. Hill, *J. Am. Chem. Soc.*, 1976, **98**, 1269.
16 G. Valensin, T. Kushnir, and G. Navon, *J. Magn. Reson.*, 1982, **46**, 23.
17 A. Allerhand, D. Doddrell, and R. Komorski, *J. Chem. Phys.*, 1971, **55**, 189.
18 K. Dill and A. Allerhand, *J. Am. Chem. Soc.*, 1979, **101**, 4376.
19 D. E. Woessner, *J. Chem. Phys.*, 1962, **36**, 1.
20 J. H. Noggle and R. E. Schirmer, 'The Nuclear Overhauser Effect,' Academic Press, New York, 1971.
21 J. Tropp, *J. Chem. Phys.*, 1980, **72**, 6035.
22 J. Feeney, *J. Magn. Reson.*, 1976, **21**, 473.
23 J. Shaw and G. W. Everett Jr., *J. Inorg. Biochem.*, 1982, **17**, 305.

Paper 9/02494H
Received 14*th June* 1989
Accepted 26*th September* 1989